AD-A129 418 ELECTRON EXCITATION OF FREE-FREE RADIATION IN ARGON AND 1/1
OF VIBRATIONAL ST..(U) NATIONAL BUREAU OF STANDARDS
BOULDER CO QUANTUM PHYSICS DIV A V PHELPS ET AL.
UNCLASSIFIED APR 83 AFWAL-TR-83-2018 F/G 20/7 NL

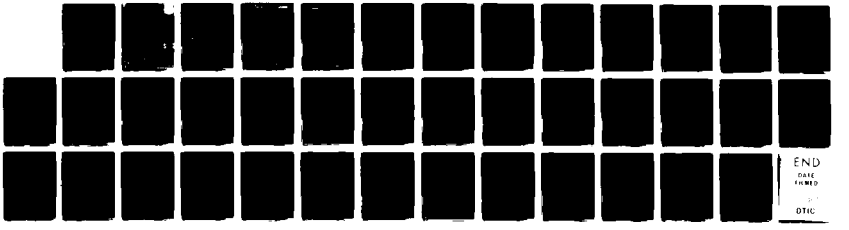

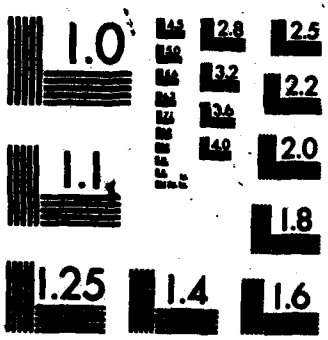

AFWAL-TR-83-2018

ELECTRON EXCITATION OF THIRD-POSITIVE RADIATION IN NITROGEN AND OF VIBRATIONAL STATES OF H_2, D_2 AND O_2

A. V. PHELPS and S. J. BUCKMAN

QUANTUM PHYSICS DIVISION
U.S. BUREAU OF STANDARDS
BOULDER, CO 80303

April 1983

FINAL REPORT FOR PERIOD OCTOBER 1981 - SEPTEMBER 1982

AERO PROPULSION LABORATORY
AIR FORCE WRIGHT AERONAUTICAL LABORATORIES
AIR FORCE SYSTEMS COMMAND
WRIGHT-PATTERSON AIR FORCE BASE, OHIO 45433

NOTICE

When Government drawings, specifications, or other data are used for any purpose other than in connection with a definitely related Government procurement operation, the United States Government thereby incurs no responsibility nor any obligation whatsoever; and the fact that the government may have formulated, furnished, or in any way supplied the said drawings, specifications, or other data, is not to be regarded by implication or otherwise as in any manner licensing the holder or any other person or corporation, or conveying any rights or permission to manufacture, use, or sell any patented invention that may in any way be related thereto.

This report has been reviewed by the Office of Public Affairs (ASD/PA) and is releasable to the National Technical Information Service (NTIS). At NTIS, it will be available to the general public, including foreign nations.

This technical report has been reviewed and is approved for publication.

ALAN GARSCADDEN
Project Engineer
Energy Conversion Branch

PAUL R. BERTHEAUD
Chief, Energy Conversion Branch
Aerospace Power Division
Aero Propulsion Laboratory

FOR THE COMMANDER

JAMES D. REAMS
Chief, Aerospace Power Division
Aero Propulsion Laboratory

"If your address has changed, if you wish to be removed from our mailing list, or if the addressee is no longer employed by your organization please notify AFWAL/POOC-3 W-PAFB, OH 45433 to help us maintain a current mailing list".

Copies of this report should not be returned unless return is required by security considerations, contractual obligations, or notice on a specific document.

UNCLASSIFIED
SECURITY CLASSIFICATION OF THIS PAGE (When Data Entered)

REPORT DOCUMENTATION PAGE

1. REPORT NUMBER: AFWAL-TR-83-2018	2. GOVT ACCESSION NO: AD-A129418
3. RECIPIENT'S CATALOG NUMBER	
4. TITLE (and Subtitle): Electron Excitation of Free-Free Radiation in Argon and of Vibrational States of H_2, D_2 and O_2	5. TYPE OF REPORT & PERIOD COVERED: Final Report for Period Oct 81 - Sep 82
	6. PERFORMING ORG. REPORT NUMBER
7. AUTHOR(s): A. V. Phelps and S. J. Buckman	8. CONTRACT OR GRANT NUMBER(s): MIPR FY1455-81-00626; MIPR FY1455-82-80604
9. PERFORMING ORGANIZATION NAME AND ADDRESS: Quantum Physics Division, U.S. Bureau of Standards, Boulder, CO 80303	10. PROGRAM ELEMENT, PROJECT, TASK AREA & WORK UNIT NUMBERS: 23018208
11. CONTROLLING OFFICE NAME AND ADDRESS: Aero Propulsion Laboratory (AFWAL/POOC), Air Force Wright Aeronautical Laboratories (AFSC), Wright-Patterson Air Force Base, Ohio 45433	12. REPORT DATE: April 1983
	13. NUMBER OF PAGES: 32
14. MONITORING AGENCY NAME & ADDRESS (if different from Controlling Office)	15. SECURITY CLASS. (of this report): Unclassified
	15a. DECLASSIFICATION/DOWNGRADING SCHEDULE

16. DISTRIBUTION STATEMENT (of this Report)

Approved for public release; distribution unlimited

17. DISTRIBUTION STATEMENT (of the abstract entered in Block 20, if different from Report)

18. SUPPLEMENTARY NOTES

19. KEY WORDS (Continue on reverse side if necessary and identify by block number)

Argon, Oxygen, Hydrogen, Electrons, Radiation, Excitation Coefficient, Free-free Radiation, Vibration, Infrared

10 to the minus 21 st power

20. ABSTRACT (Continue on reverse side if necessary and identify by block number)

Final measurements are reported for the production of free-free emission by low energy electrons in argon. Absolute intensity measurements were made at 500, 650 and 1000 nm. The electric field to gas density ratio was varied from 0.25 to 10 $\times 10^{-21}$ Vm^2, corresponding to mean electron energies from 1.2 to 5.4 eV. The experimental results agree well with theoretical values calculated from cross sections for momentum transfer collisions determined by other techniques. Measurements of vibrational excitation of O_2, H_2 and D_2 (cont'd. over)

DD FORM 1473

UNCLASSIFIED
SECURITY CLASSIFICATION OF THIS PAGE (When Data Entered)

20. ABSTRACT (continued)

were initiated using the collisional transfer of energy from a homonuclear molecule to a heteronuclear molecule, i.e. CS_2 for O_2 and CO_2 or CO for H_2 and D_2. Signals were observed using D_2 and CO_2.

PREFACE

This work was performed in the Quantum Physics Division, U.S. Bureau of Standards, at the Joint Institute for Laboratory Astrophysics under MIPR FY1455-81-00626 and MIPR FY1455-82-H0604. This work was performed during the period October 1981 through September 1982 under Project 2301 Task S2, "Plasma Research, Gas Discharge and Laser Plasmas." The Air Force contract manager was Dr. Alan Garscadden, Energy Conversion Branch, Aero Propulsion Laboratory, WPAFB, OH 45433.

TABLE OF CONTENTS

LIST OF ILLUSTRATIONS

SECTION I

INTRODUCTION

The measurements described in this report are concerned with the production of radiation and of vibrationally excited molecules when electrons move through gases under the influence of an electric field. First, we describe our measurements of the production of photons as the result of the collisions of electrons with argon atoms in what is known as the free-free or bremsstrahlung process. Second, we discuss progress during this contract period toward the measurement of coefficients for the vibrational excitation of the homonuclear molecules H_2, D_2 and O_2.

The measurements of the coefficients for the production of free-free radiation in the collisions of electrons with argon atoms were completed and the results were submitted for publication during this contract period. Rather than rework this material for this report, we have incorporated the manuscript of this paper as Sec. II. Briefly, the results of this work are that we have verified to a much higher degree of accuracy -- 15% -- than previously the utility of a simple theory for predicting the magnitude of free-free radiation at mean electron energies between 1 and 5 eV. As a result of this verification one can confidently use free-free emission as a diagnostic for moderate energy plasmas, such as those occurring in high power switching devices, charged particle beam propagation, rare gas-halide lasers, and in the ionosphere. If this same theoretical model is used to interpolate between our results (Sec. II) and high energy theory and experiment

(Reference 1), the cross section for the emission of free-free radiation at 500 nm by electrons in argon is that shown in Fig. 1. Figure 1 also shows the application of this theory to helium and to nitrogen (References 1, 2).

Section III of this report describes the results of work during FY 82 on the development of techniques for the measurement of excitation coefficients for the production of vibrationally excited H_2, D_2 and O_2 by low energy electrons. Successful measurements of the vibrational excitation of D_2 and H_2 using these techniques were made a few weeks after the end of the FY 82 report period.

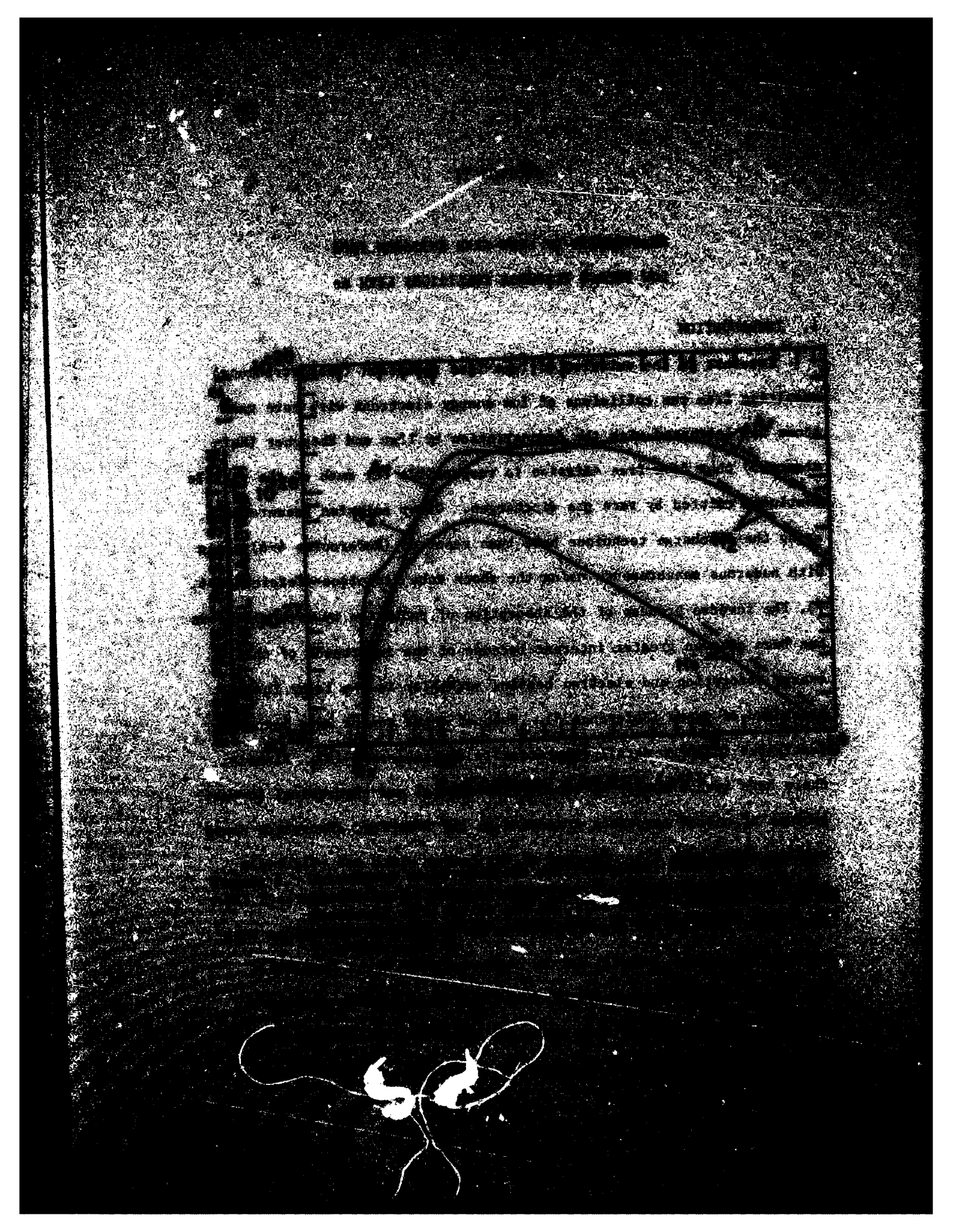

SECTION II

MEASUREMENT OF FREE-FREE EMISSION FROM LOW ENERGY ELECTRON COLLISIONS WITH Ar

1. INTRODUCTION

Interest in the emission of free-free radiation (bremsstrahlung) resulting from the collisions of low energy electrons with rare gas atoms has increased with the demonstration by Pfau and Rutscher (Reference 3) that free-free emission is responsible for much of the visible continuum emitted by rare gas discharges. Other emission measurements using the discharge technique have been reported (References 4-6) along with numerous measurements using the shock tube technique (References 6, 7). The inverse process of the absorption of radiation by free electrons has been of even greater interest because of the importance of this energy absorption and electron heating mechanism in the laser induced breakdown of gases (Reference 8). Both of these topics have been investigated in great detail theoretically (References 8-15). Finally, there have been a number of recent experimental and theoretical investigations of narrow resonance structure in the free-free absorption cross section (Reference 15). Because of the narrow width and relatively small integrated contribution of these resonances to the averaged free-free cross sections of significance in our relatively low energy resolution experiments, we will not be concerned with these features.

The present measurements of free-free emission were carried out using the electron drift tube technique which we have used previously (References 16-18) for measurements of excitation coefficients for

weakly radiating states of molecules. In these experiments a photoelectrically produced electron current drifts through the gas under the action of a spatially uniform, time modulated electric field. About one in 10^8 collisions of the electrons with the gas atoms results in the emission of a visible photon. A small fraction (~ 1 in 10^4) of these photons is selected by wavelength and reaches the sensitive area of the detector. The absolute photon flux is compared with that from a standard lamp and the ratio is used to calculate the excitation coefficient. The principal advantage of the present technique over the discharge technique used in previous experiments (References 3-6) is that the electric field E and gas density N can be easily varied and accurately determined and that the theory of the experiment need not take into account electron-electron and electron-ion collisions (Reference 19). A disadvantage of the drift tube technique is that the emitted intensities are about 10^4 smaller than in a typical discharge experiment.

2. THEORY OF EXPERIMENT

In this section we briefly review the results of theoretical calculations of free-free radiation and of the excitation coefficients which are relevant to this experiment. We then derive the equations necessary to relate the observed signals to the excitation coefficients.

a. Free-free emission theory

For our purposes it is convenient to divide the free-free emission continuum into a number of spectral bands of frequency width $d\nu$ and to regard the collision process leading to emission of radiation in this

band as an inelastic collision between the electrons and gas atoms. The spectral intensity I_ν in units of photons per unit volume and per unit frequency interval and per unit time is given by (Reference 3)

$$I_\nu d\nu = n_e N \frac{d\nu}{\nu} \int^\infty v\, Q_{ff}(\varepsilon, h\nu)\varepsilon^{1/2} f(\varepsilon) d\varepsilon \equiv k_{ff}(\nu) n_e N \frac{d\nu}{\nu} \quad . \qquad (1)$$

Here n_e and N are the electron and neutral atom or molecule densities, v and ε are the electron speed and energy, $f(\varepsilon)$ is the normalized electron energy distribution and $Q_{ff}(\varepsilon, h\nu)$ and k_{ff} are the cross section and rate coefficient per fractional band width $d\nu/\nu$ for emission of a photon of energy $h\nu$ by the free-free process. Figure 2 shows theoretical calculations of the cross section per fractional bandwidth $Q_{ff}(\varepsilon, h\nu)$ as obtained by a variety of theoretical approaches for $h\nu = 1.78$ eV. The dashed and solid curves are from the quantum mechanical calculations of Ashkin (Reference 12) and of Geltman (Reference 13). The solid circles are our calculations using the very simple formula of Kas'yanov and Starostin (Reference 10) for $h\nu \ll \varepsilon$ and momentum transfer cross sections used previously (Reference 17) for Ar. This formula is

$$Q_{ff}(\varepsilon, h\nu) = \frac{4}{3\pi} \frac{\alpha^3}{Ry} \frac{(\varepsilon - h\nu/2)(\varepsilon - h\nu)^{1/2}}{\varepsilon^{1/2}} Q_m(\varepsilon)$$

$$= 1.211 \times 10^{-8} \left(1 - \frac{h\nu}{2\varepsilon}\right)\left(1 - \frac{h\nu}{\varepsilon}\right)^{1/2} \varepsilon\, Q_m(\varepsilon) \quad , \qquad (2)$$

where α is the fine structure constant (1/137), Ry is the Rydberg (13.6 eV), ε is in eV, and $Q_m(\varepsilon)$ is the cross section for momentum transfer collisions of electrons with the atom or molecule. Calculations made using the formula of Holstein (Reference 11) and the total and momentum transfer cross sections of Hayashi (Reference 2) are shown

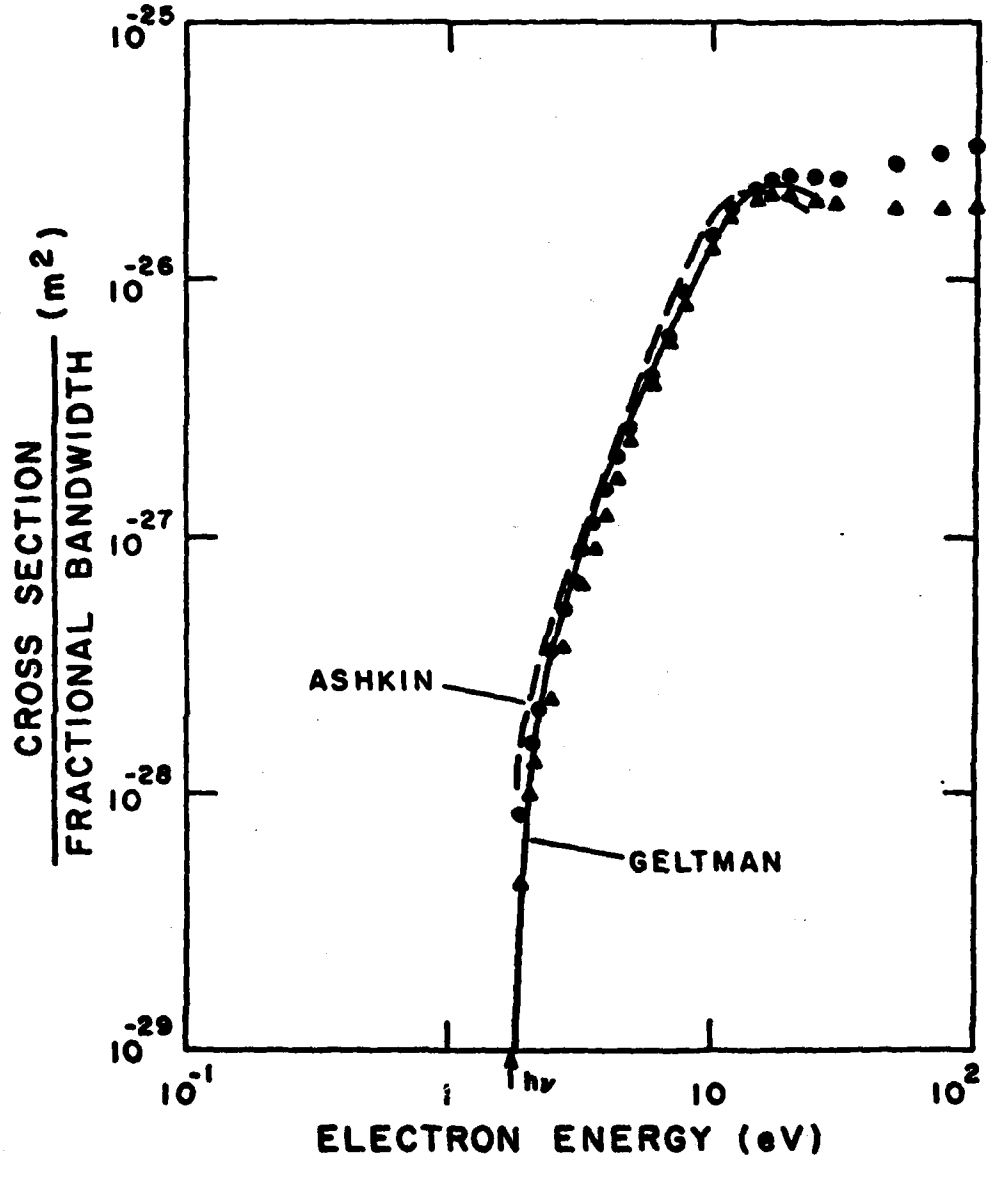

Figure 2. Theoretical cross section per fractional bandwidth for the emission of 1.78 eV photons vs. electron energy. The solid and dashed curves are from Geltman (Reference 13) and Ashkin (Reference 12), respectively. The circles and squares are our calculations based on the formulas of Kas'yanov and Starostin (Reference 10) and of Holstein (Reference 11), respectively.

by the triangles in Fig. 2. The differences among the various theoretical cross sections shown in Fig. 2 are less than 30% over most of the electron energy range. Most of the difference between the cross section calculated using Eq. (2) and those calculated using Holstein's formula results from the fact that in Eq. (2) the Q_m is evaluated at ε, whereas in Holstein's formula the cross sections are evaluated at $\varepsilon - h\nu/2$. The differences among the cross sections are larger near threshold, e.g. a factor of 3 at 2 eV for Ashkin's results vs. our application of Holstein's formula shown in Fig. 2. The large differences between the calculations at electron energies above 20 eV are caused by differences in the momentum transfer cross sections used in Reference 17 and those of Hayashi (Reference 2). As we shall see, our experiments are not sensitive to cross sections at either of these extremes of energy. The cross sections predicted using the older formula of Firsov and Chibisov (Reference 9) and the total scattering cross sections of Hayashi are much larger than the values shown in Fig. 2.

Excitation coefficients for free-free emission were calculated from the cross sections generated by Eq. (2), by Geltman (Reference 13) and by the Holstein formula (Reference 11). The electron energy distributions for Eq. (1) are calculated using the numerical procedures of Frost and Phelps (Reference 21) and the cross sections discussed by Tachibana and Phelps (Reference 16). The calculated free-free emission coefficients will be presented with the experimental results in Sec. II.4. Although not directly useful in this paper because of the assumed Maxwellian electron energy distribution, we note that there is good agreement among a number of theoretical calculations (References 6, 13,

14) of free-free emission and absorption coefficients for electrons in Ar. The Maxwellian electron energy distributions are appropriate to shock tube experiments (Reference 7) and to discharge experiments at high fractional ionization (Reference 4).

It is important to keep in mind that throughout this paper we have not followed the usual convention of expressing the free-free emission in terms of a spectral intensity, i.e., cross section or excitation coefficient per unit spectral bandwidth, but rather have defined cross sections and rate coefficients per fractional bandwidth. This unconventional formulation has the advantages of yielding numbers which are independent of units used to measure bandwidth and of yielding cross sections and excitation coefficients which are readily compared with cross sections and excitation coefficients for the production of excited states which emit lines or molecular bands. In our experiments the fractional bandwidth of the detection system is typically 0.1.

b. Model of experiment

The signal produced by the photon detector S_{ff} is obtained by integrating Eq. (1) over the drift tube volume V and over frequency ν, taking into account the optical system and detector characteristics, i.e.,

$$S_{ff} = \iint \frac{d\nu}{\nu} dV \, k_{ff}(\nu) n_e N f_w(\nu) D(\nu) f_i(\nu) \frac{\Delta\Omega_c}{4\pi} \eta(\underline{r}) \quad , \qquad (3)$$

where $f_w(\nu)$ is the fractional transmission of the windows between the collision chamber and the detector, $D(\nu)$ is the responsitivity per photon of the detector, amplifier and recording system as a function of

ν, $f_i(\nu)$ is the fractional transmission of the interference or other filter inserted between the collision chamber and the detector, $\Delta\Omega_c$ is the solid angle of the detector as seen from the center of the collision chamber, and $\eta(\underline{r})$ is the efficiency of the detection system at various points in the collision chamber relative to that at the center of the chamber (Reference 16).

Equation (3) can be rewritten as

$$S_{ff} = \frac{N\Delta\Omega_c}{4\pi} \int_0^\infty f_w(\nu) k_{ff}(\nu) D(\nu) f_i(\nu) \frac{d\nu}{\nu} \times \int_V n_e \eta(\underline{r}) dV \quad . \qquad (4)$$

We define a geometrical factor G_{ff} by the relation

$$G_{ff} = \int_V n_e \eta(\underline{r}) dV / \int_V n_e \, dV \quad . \qquad (5)$$

We note that G_{ff} is equal to the G factor defined by Lawton and Phelps (Reference 16) in the limit of no diffusion. Since ionization and attachment can be neglected in the present experiments at low E/N in pure Ar, the electron density n_e can be assumed to be independent of position in the electric field direction. If, as in previous papers (References 16, 17), we neglect the effects of radial variations in the electron density, then the expression for G_{ff} reduces to a constant equal to the average of $\eta(\underline{r})$ over the active portion of the drift tube. This constant was 0.97 for the infrared detector and 0.80 for the photomultiplier detector.

In the usual case of a slow variation in f_w, $k_{ff}(\nu)$ and $D(\nu)$ with ν compared to that of $f_i(\nu)$, the integral over ν in Eq. (4) can be written as $f_w(\nu_i)k_{ff}(\nu_i)D(\nu_i)\langle f_i\rangle \Delta\nu$. Here $\langle f_i\rangle\Delta\nu$ is the "area" under the

filter transmission curve and ν_i is the photon frequency at the peak of the transmission of the interference filter. Equation (4) can now be approximated by

$$S_{ff} = \frac{N\Delta\Omega_c G_{ff}}{4\pi} \frac{iL}{ew_e} f_w(\nu_i) k_{ff}(\nu_i) D(\nu_i) \langle f_i \rangle \frac{\Delta\nu}{\nu} \quad , \qquad (6)$$

where L is the separation of the cathode and anode of the drift tube, i is the current through the drift tube and e and w_e are the electron charge and drift velocity. Note that because of the absence of significant attachment or ionization, the q factor of Reference 16 is equal to unity and so is omitted from Eq. (6). Measurements at significantly higher E/N would require that corrections be made for ionization. From Eq. (6) we note that since the free-free emission signal increases with the fractional bandwidth $\Delta\nu/\nu$ of the detection system, one should use a wide band width interference filter or a very low resolution monochromator for wavelength selection.

The reference signal S_r reaching the detector from the reference, i.e., the blackbody or the calibrated tungsten strip lamp, is given by

$$S_r = \Delta\Omega_r a_r \int_0^\infty f_r(\nu) f_w(\nu) \epsilon(\nu) B(\nu) D(\nu) f_i(\nu) d\nu \quad , \qquad (7)$$

where $\Delta\Omega_r$ is the solid angle of the detector as seen from a limiting aperture (Reference 16) of area a_r, $f_r(\nu)$ is the transmission of the windows between the reference source and the collision chamber, $\epsilon(\nu)$ is the emissivity of the reference source, $B(\nu)d\nu$ number of photons per second emitted by a blackbody per unit of surface and per unit solid angle. As discussed in Reference 16, the reference sources were large

enough to completely fill their limiting apertures as seen from the detector.

Using Eqs. (4), (5) and (7) rather than Eq. (6) for greater accuracy, we find that the ratio of the free-free emission signal to the reference signal is

$$\frac{S_{ff}}{S_r} = \frac{N\Delta\Omega_c G_{ff}}{4\pi\Delta\Omega_r a_r} \frac{iL}{ew_e} \frac{\int_0^\infty f_w(\nu)k_{ff}(\nu)D(\nu)f_i(\nu)d\nu/\nu}{\int_0^\infty f_r(\nu)f_w(\nu)\epsilon(\nu)B(\nu)D(\nu)f_i(\nu)d\nu} \quad . \tag{8}$$

If we define a free-free excitation coefficient $\alpha_{ff}(\lambda_i)$ by

$$\alpha_{ff}(\lambda_i) = k_{ff}(\nu_i)N/w_e \quad , \tag{9}$$

then

$$\frac{\alpha_{ff}(\lambda_i)}{N} = \frac{C_{ff}\, S_{ff}}{G_{ff} i N S_r} \quad , \tag{10}$$

where here λ_i is taken to be the mean wavelength transmitted by interference filter and

$$C_{ff}(\lambda_i) = \frac{4\pi\Delta\Omega_r e a_r}{\Delta\Omega_c L} \frac{\int_0^\infty f_r(\lambda)f_w(\lambda)\epsilon(\lambda)B'(\lambda)D'(\lambda)f_i(\lambda)d\lambda}{\int_0^\infty f_w(\lambda)f_i(\lambda)\left[\frac{k_{ff}(c/\lambda)}{k_{ff}(c/\lambda_i)}\right]D'(\lambda)\frac{hc}{\lambda^2}d\lambda} \quad . \tag{11}$$

Here

$$D'(\lambda) = D(\nu)/h\nu \quad \text{and} \quad h\nu B(\nu)d\nu = B'(\lambda)d\lambda \quad .$$

Equation (11) was used for analyzing the data presented in this paper. We note that the formula for determining $\alpha_{ff}(\lambda_i)/N$ from the experimental data, i.e., Eq. (10), is very much like Eq. (17) of Lawton and Phelps (Reference 16) for determining α_b/N for the $O_2(b^1\Sigma)$ metastables.

3. EXPERIMENTAL APPARATUS AND PROCEDURE

A schematic of the drift tube technique used for determination of the free-free excitation coefficients is shown in Fig. 3. Ultraviolet radiation from a continuously operating 100 W high pressure mercury lamp is passed through broad band interference filters with maximum transmission at 190 nm and then through a quartz window coated on the inside with a semi-transparent, cathode film of evaporated Pd-Au alloy. The resulting photoelectrons enter the parallel plate drift tube filled with Ar at densities from 3 to 15 × 10^{24} atom/m^3. The anode voltage is modulated so as to periodically apply a known electric field E and so produce electrons with a modulated mean energy. The photons emitted in the free-free transitions are detected with a photoconductive detector for the infrared or with a photomultiplier for visible wavelengths. The free-free emission signal is compared with the signal from a hollow cavity blackbody for the infrared and with a calibrated tungsten ribbon lamp for the visible wavelengths.

The drift tube used in these experiments and shown in the schematic of Fig. 3 is the same as the one used previously (References 16-18) to measure excitation in molecular gases. The electrode spacing was 38.4 mm and the cathode diameter was 60 mm. The accelerating voltage ranged from 60 to 3100 V and the total current in the on-period was 0.02 to 0.09 μA. Measurements are reported at total gas densities of 3 to 15 × 10^{24} m^{-3}. Argon of nominal 99.999% purity was fed into the tube directly from a high pressure cylinder.

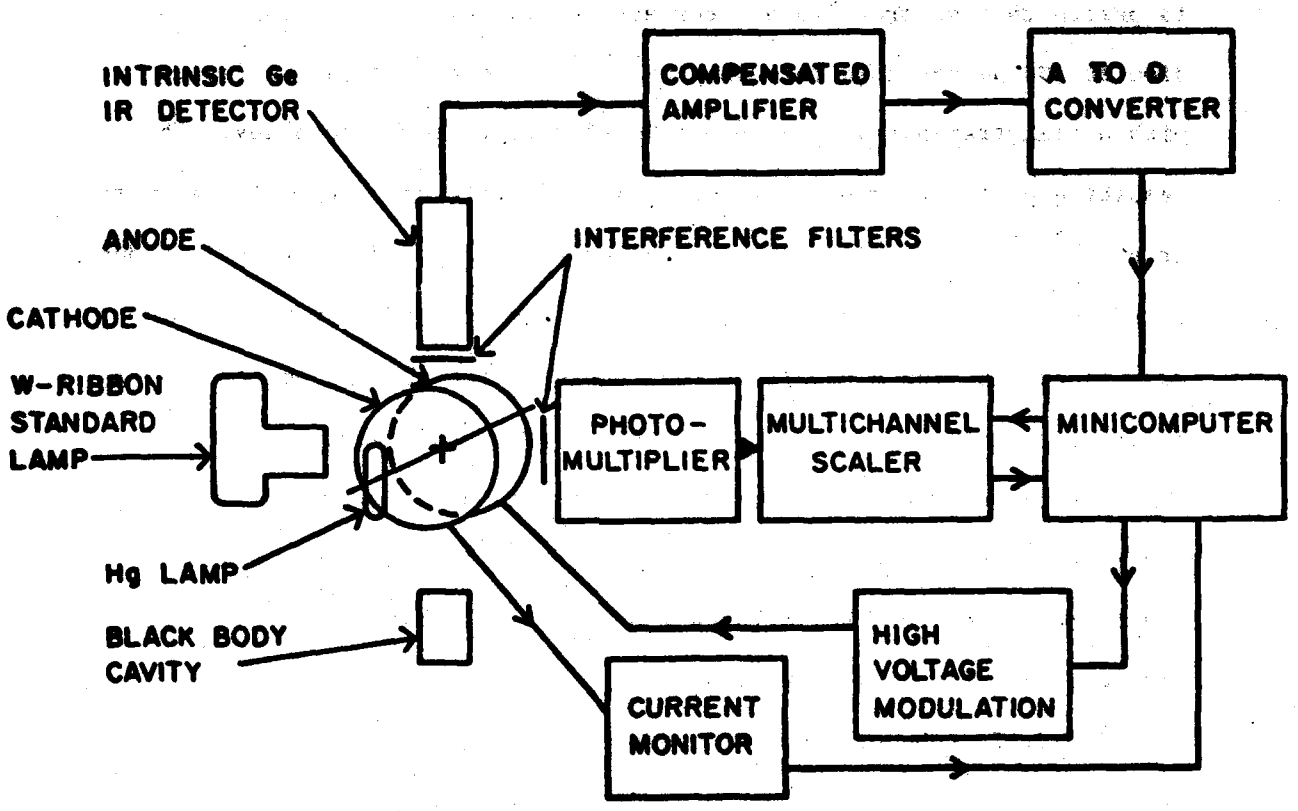

Figure 3. Schematic of experiment. Note that the centers of the semi-transparent cathode, the anode, the drift tube and the Hg lamp are on an axis perpendicular to the plane of the reference sources and the detectors.

a. Infrared system

The measurements at 1.3 μm were made with a period of the zero-based square wave voltage applied to the anode of 25 s as in the measurements of the 1.27 μm emission from the $a^1\Delta_g$ state of O_2. This data recording period was followed by a dead time of 15 s for computer processing of the data. The liquid-N_2 cooled, intrinsic germanium detector had responsivity and NEP (noise equivalent power) of 7×10^9 V/W and 1×10^{-15} WHz$^{-1/2}$, respectively, at 1.3 μm. The signal from the "dc" output of the detector for step function infrared input signal consists of rapidly and slowly rising components, the time constants of which were about 10 ms and 3 s, respectively. As described in Reference 17, this problem was overcome by using an amplifier containing differentiation and addition circuits which compensate for the 3 s response and partially compensate for the 10 ms response. The compensation circuits were adjusted for a square wave output signal using the chopped signal from the blackbody as an input signal.

A minicomputer was used as a data acquisition and analyzing system. The signal from the compensated amplifier was sampled every 0.1 s using an analog- to-digital converter. A set of data was stored in the computer and then analyzed (Reference 17) to reject spikes due to cosmic rays. Sixteen to thirty-two sets of data were additively accumulated and averaged in the computer.

The measurement of the sensitivity of the detection system for infrared radiation emitted from the center of the collision chamber was made using a blackbody source mounted on the opposite side of the drift tube from the detector. A chopper in front of the source modulated the

blackbody emission with a period of 20 s. An aperture of 1.50 mm diameter was placed in front of the source 0.47 m from the detector so as to reduce the blackbody signal. When the temperature of the source was 490 K the intensity at the detector was comparable to that observed for the free-free emission and was large compared to the thermal background signal. The spatial variation of the detection efficiency $\eta(\underline{r})$ was measured using a small diffuse light source which was scanned over the drift region as described in Reference 17.

b. Visible wavelength system

The detection system and reference light source for the measurements of free-free emission at 500 and 650 nm was a modification to that described by Lawton and Phelps (Reference 16). An improved photon counting system was used to integrate the photomultiplier signals during the on and off times for the high voltage applied to the drift tube. The photomultiplier counts and the digitized average cathode current were transferred to the minicomputer after a preset time interval. An interference filter with 68% transmission and a band pass of 68 nm FWHM was used for the measurements reported for 500 nm. Measurements at 650 nm were made using an interference filter with 65% peak transmission and a band pass of 33 nm FWHM. As pointed out previously (Reference 16), the final results are insensitive to the magnitude of the interference filter transmission. The filter characteristics were measured separately using a commercial spectrophotometer. A multi-alkali photomultiplier in a UV transmitting envelope with a slowly varying quantum efficiency between 250 and 800 nm was used with these filters. The

principal difficulty encountered in these measurements was that of the calibration of the neutral density filters used to reduce the signal from the standard lamp to values in the linear range of the photon counting system.

We estimate an uncertainty of ±20% for the resultant measured excitation coefficients for both the infrared and visible wavelengths. The significant changes in these estimates from those of Reference 16 are the absence of a contribution to the uncertainty from a radiative lifetime, a more accurate measurement of the aperture area (±4%), and a more accurate determination of the electron current (±5%).

4. FREE-FREE EMISSION DATA

In this section we summarize the results of measurements of the free-free emission coefficients for electrons in Ar. Figure 4 shows an example of the infrared emission signals which led us to the conclusion that the drift tube technique could be used to measure free-free emission coefficients. This waveform was obtained during measurements of $O_2(a^1\Delta)$ production in a mixture of 0.05% O_2 in Ar at a total gas density of 10^{25} m^{-3} and an E/N of 3×10^{-21} Vm^2. The exponentially rising and falling portions of this waveform are interpreted as emission from $O_2(a^1\Delta)$ molecules at 1.27 μm and yield excitation coefficients consistent with those reported in References 16 and 17. When the exponentially varying portions are subtracted from the observed waveform one is left with a rectangular waveform which we interpret as free-free emission emitted in collisions between electrons and argon atoms.

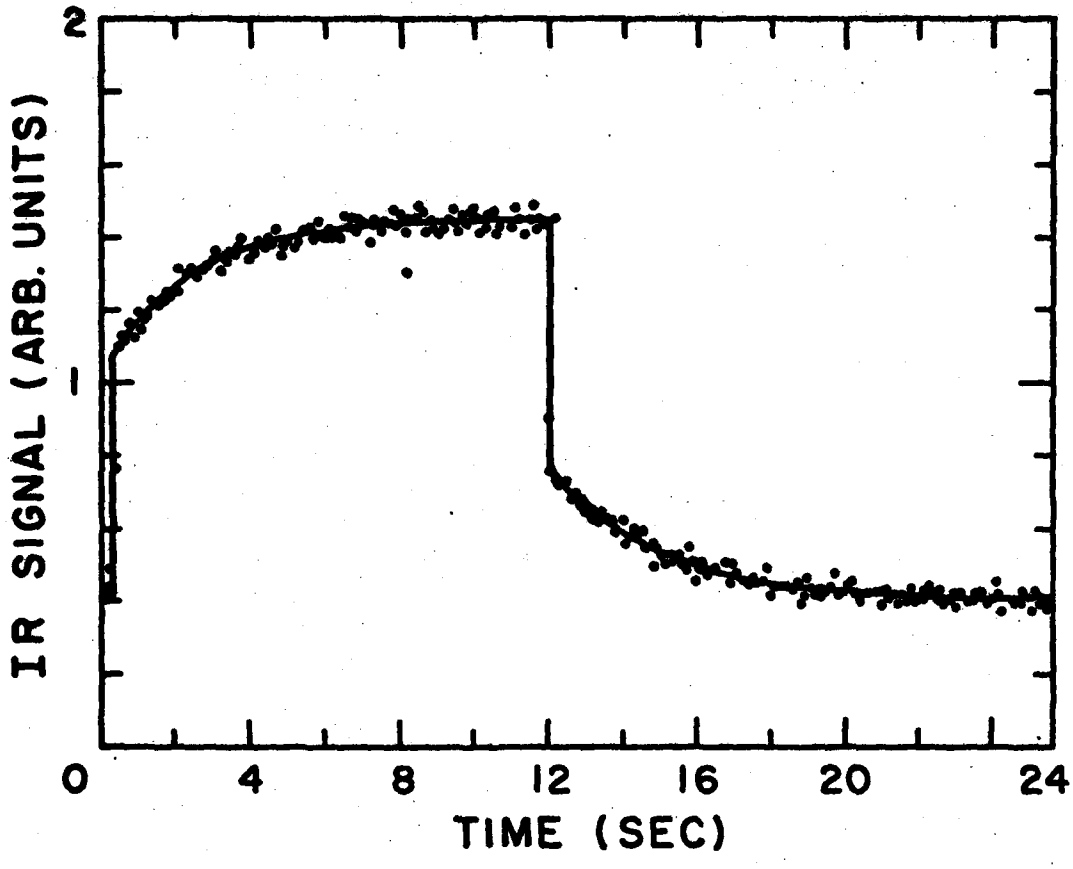

Figure 4. Infrared emission transient near 1.3 μm from 0.05% O_2 in Ar.

This interpretation is supported by the fact that in pure Ar only the rectangular component of the waveform was observed. Although one expects the free-free emission signal to follow the rapid changes in the electron density, we made no effort to observe he free-free emission with a time resolution better than the 0.1 s value normally used in the $O_2(a^1\Delta)$ experiments. Winkler, Michel and Wilhelm (Reference 21) have observed changes in the free-free emission from afterglows in Ne and Ar on a microsecond time scale. The principal clues to the identity of the signal were the slow variation of the signal with E/N and with wavelength, as discussed in the remainder of this section.

The free-free emission coefficients for pure Ar at wavelengths near 1.3 μm are calculated from the observed magnitude of the infrared signal using Eqs. (10) and (11). The averages of several runs are shown as a function of E/N by the squares in Fig. 5. Similarly, the triangles and the circles of Fig. 5 show the averages of results of measurements near 500 and 650 nm, respectively. Plots of the free-free emission coefficient versus wavelength for E/N values of 3×10^{-21} Vm^2 (squares) and 2×10^{-21} Vm^2 (triangles) are shown in Fig. 6. Note that when appropriate corrections are made for the effects of attachment, the free-free emission data of Fig. 4 and other data from O_2-Ar mixtures obtained during measurements at 1.3 μm are consistent with the 1.3 μm data shown in Fig. 5.

The solid curves of Figs. 5 and 6 are the result of calculations of free-free emission coefficients which we have made using Eq. (2) for the free-free emission cross section and the electron energy distributions

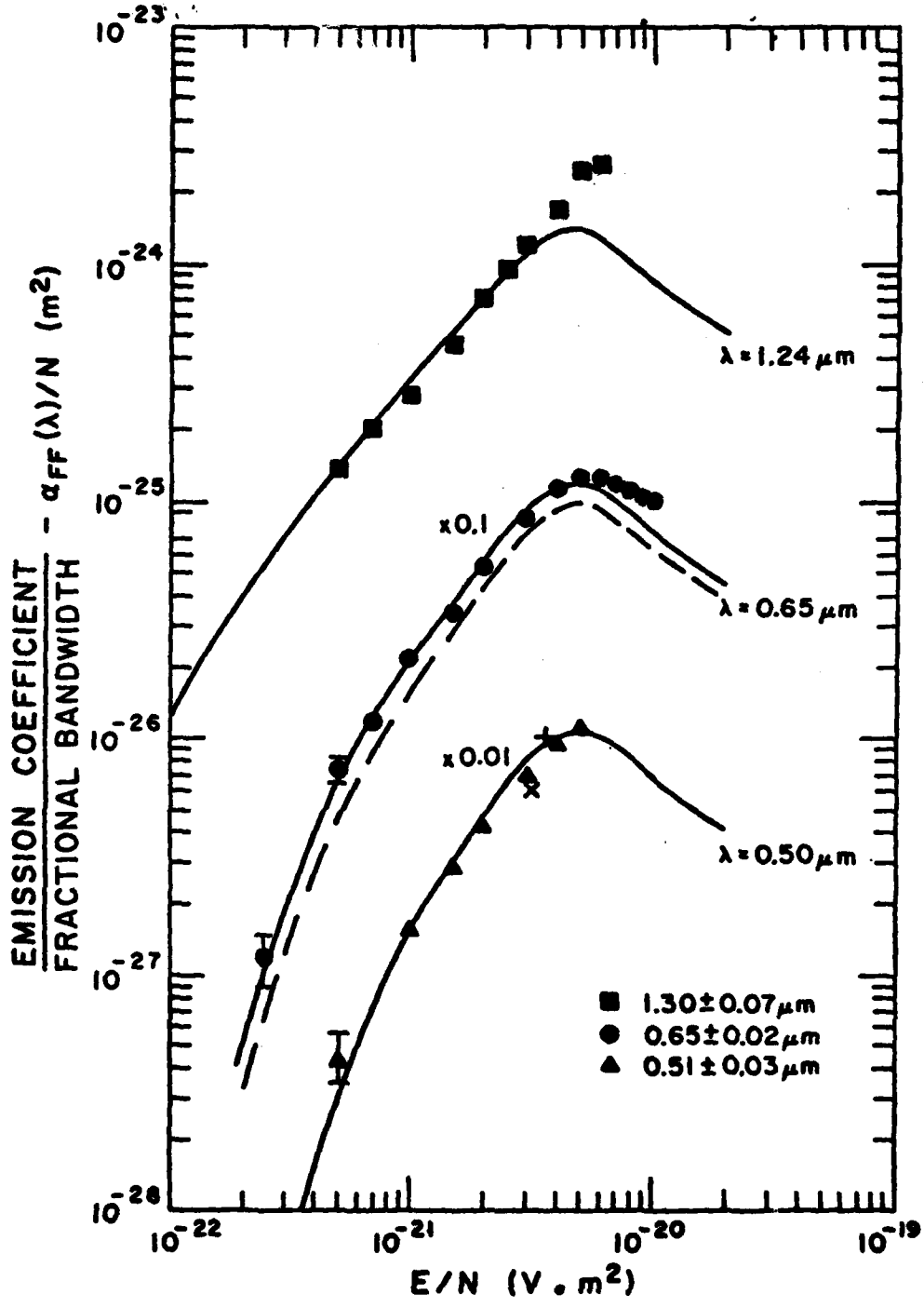

Figure 5. Free-free emission coefficient per fractional bandwidth for electrons in argon vs. E/N. The error bars shown at low E/N for 500 and 600 nm are the statistical uncertainties associated with photon counting. The x and + are representative data from References 4 and 5, respectively. The solid curves calculated values obtained using Eqs. (1) and (2). The dashed curve shows results calculated using Holstein's formula (Reference 11).

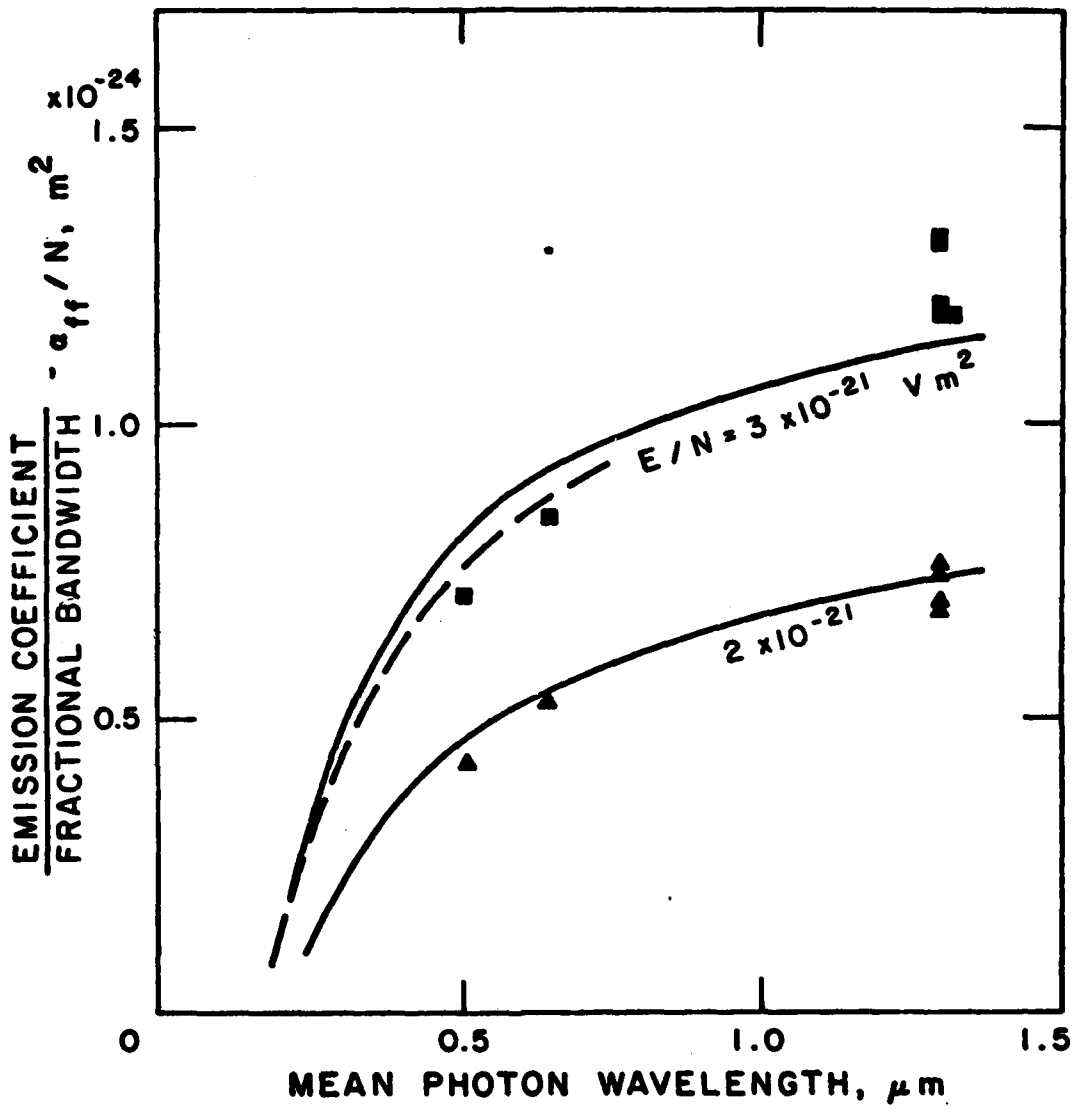

Figure 6. Wavelength dependence of free-free emission coefficient per fractional bandwidth for electrons in Ar. The solid curves are our calculated values, while the dashed curve is from Pfau, Rutscher and Winkler (Reference 22). The triangles and squares are our experimental results for E/N values of 2 and 3×10^{-21} Vm^2, respectively.

which we have calculated. For this purpose, it is convenient to write Eq. (1) as

$$\frac{\alpha_{ff}}{N} = \frac{k_{ff}}{w_e} = \frac{1}{w_e}\left(\frac{2}{m}\right)^{1/2} \int_{h\nu}^{\infty} \varepsilon Q_{ff}(\varepsilon) f(\varepsilon) d\varepsilon \quad . \tag{12}$$

Here α_{ff} is the number of free-free photons emitted per unit distance of electron drift and per fractional band width. According to Eq. (12) the normalized excitation coefficient is expected to be independent of the argon density. Our electron energy distributions were calculated using the electron-Ar collision cross section data discussed in Sec. II.3 and in Reference 17. The dashed curve for λ = 650 nm of Fig. 5 was calculated using the $Q_{ff}(\varepsilon, h\nu)$ values for λ = 650 nm calculated using the theory of Holstein. In this case the momentum transfer cross sections of Hayashi (Reference 2) were used in the calculation of $f(\varepsilon)$, although the $Q_m(\varepsilon)$ values of References 17 and 2 agree for $\varepsilon < 3$ eV and differ by less than 10% for $\varepsilon < 15$ eV. The α_{ff}/N values calculated from the theoretical cross sections of Geltman are not shown in Fig. 5 since they differ from the results obtained with Eq. (1) by less than about 5% for $E/N > 0.3 \times 10^{-21}$ Vm^2. The decrease in the calculated α_{ff}/N values for E/N greater than 4×10^{-21} Vm^2 is the result of an increase in the slope of the drift velocity vs E/N data as well as a decrease in the slope of k_{ff} vs. E/N at E/N where inelastic collisions are important (References 16, 22). The calculated mean electron energies vary from 1.2 eV at $E/N = 2.5 \times 10^{-22}$ Vm^2 to 5.4 eV at $E/N = 1 \times 10^{-20}$ Vm^2. The dashed curve of Fig. 6 was obtained by interpolation of graphs of calculations by Pfau, Rutscher and Winkler (Reference 22). The lower emission coefficients obtained by these authors compared to those we calculate at the

same E/N appear to be the result of their use of somewhat larger $Q_m(\varepsilon)$ values for electron-Ar collisions with a resultant lower mean electron energy and lower α_{ff}/N.

For E/N below 3×10^{-21} Vm^2, the agreement between experiment and the theory of Kas'yanov and Starostin (Reference 10) as shown by the solid curves, is within ±15% or the statistical uncertainty of the data in spite of the fact that the hν values are comparable with the photon energy. Although the theoretical curve calculated using the formula of Holstein (Reference 11) lies well outside the statistical uncertainty of our data, it is just within the confidence limits we have assigned to our results. The relatively large experimental values and rapid increase of the α_{ff}/N coefficients relative to theory for $\lambda = 1.3$ μm at E/N values above 4×10^{-21} Vm^2 are consistent with α/N values which we calculate for the emission of line radiation by highly excited Ar atoms. The excess of the measured signal at 650 nm at $E/N > 5 \times 10^{-21}$ Vm^2 varies much less rapidly with E/N than expected for highly excited states of Ar. Although this discrepancy may indicate an error in the values of $Q_m(\varepsilon)$ at electron energies above about 10 eV, further measurements of the spectral distribution of the radiation should be made so as to verify that the emission at the higher E/N is free-free radiation.

Absolute measurements of free-free emission signals from electrical discharges in Ar are reported for wavelengths from 300 to 500 nm by Vasileva, Zhdanova and Mnatsakanyan (Reference 5) and for 480 nm by Golubovskii, Kagan and Komarova (References 4, 23). Their results were about (75 ± 20%) and (100 ± 20%), respectively, of their theoretical values. Representative experimental data obtained by these authors

at 500 nm are shown in Fig. 5. The E/N range of their low current discharges sets the mean electron energy in the range of 4-5 eV. The agreement between experiment and theory shown for these authors is remarkably good when one considers the problems of the determination of the electron density and of the effects of gas heating on the analysis of their experimental data (Reference 23). The results of Vasileva, et al. (Reference 5) and of Rutscher and Pfau (Reference 3) also provide tests of the theoretical predictions of the wavelength dependence of the free-free emission.

5. DISCUSSION

The results presented in this paper show the usefulness of the electron drift tube technique for the measurement of free-free emission coefficients for electrons in gases. This technique makes possible measurements of free-free emission coefficients under much more accurately known experimental conditions for a wide range of mean electron energies (1.2 to 5.4 eV) than was possible using the discharge technique. The free-free emission coefficients for photon energies between 1 and 2.5 eV and for mean electron energies between 1.7 and 5.0 eV agree with theoretical predictions to within ±15%. At 650 nm and mean electron energies from 1.7 eV down to 1.2 eV the experimental and theoretical agree within the statistical uncertainty of less than ±25%, while at mean electron energies above 5.0 eV the apparent discrepancy between theory and experiment increases with electron energy. Unfortunately, the mean electron energies required to produce a measurable signal are too large

to enable us to work in the threshold electron energy range where the various theories are more easily distinguished. Measurements of free-free emission at very high densities of pure gases or absorption measurements using low mean energy electrons might make possible a choice from among the theories. Free-free emission measurements (Reference 24) at extremely high gas densities ($\sim 10^{29}$ m^{-3}) should provide data for testing theories appropriate to conditions in which the time between electron-atom collisions is comparable to the photon frequency, but under much more accurately controlled conditions than in the laser breakdown experiments (Reference 8) carried out at these densities. Such high density emission experiments should provide a valuable complement to electron mobility measurements at high gas densities where departures from the binary collision model of electron scattering may occur (Reference 25).

On the basis of the success of the simple formula for calculating free-free emission coefficients for argon, one is encouraged to recommend the use of this formula for other gases for which the momentum transfer cross section is known. Obviously, it would be desirable to test the formula against experiment for other gases, e.g., He and N_2.

SECTION III

VIBRATIONAL EXCITATION OF HOMONUCLEAR MOLECULES

The objective of these experiments is to develop and apply techniques for the measurement of coefficients of the production of vibrationally excited homonuclear molecules by low energy electrons. The molecules of particular interest are H_2, D_2, and O_2. Reliable data for the electron excitation of H_2 and D_2 molecules is essential to the accurate modeling of the role of these excited levels in negative ion sources and in hydrogen filled thyratrons and switches. Thus, it is known that the rate of negative ion formation in H_2 and D_2 is a strong function of the degree of vibrational excitation produced in an electrical discharge (Reference 26). At the present time there is about a factor of two uncertainty in the slope of the cross section near threshold for vibrational excitation of H_2 by electrons (References 27, 28). In the case of D_2, the only cross section data at energies of interest for discharges appear to be the result of an analysis of electron transport data which, for the similar case of H_2, are known to be significantly in error at the higher energies (Reference 29). The interest in vibrational excitation of O_2 arises from the fact that this process dominates the energy loss by electrons in air with mean energies between 0.2 and 1 eV, i.e., the energies of electrons predicted to be found in plasmas produced when high energy electron beams propagate stably through air. At the present time there is a factor of two discrepancy between the better of the two sets of cross section data obtained using electron

beam techniques (Reference 30) and results we have derived from electron transport data (Reference 16).

The experimental arrangement used in these measurements is identical with that used for the infrared measurements described in Sec. II, except for changes in the infrared detector and its associated amplifiers. The basic approach to the measurement of the densities of vibrationally excited homonuclear molecules is to make use of excitation transfer from the homonuclear molecule to a heteronuclear molecule which radiates in the infrared. The theory of the experiment (Reference 31) shows that the largest signals will be obtained when the vibrational energies of the two molecules are in close resonance, as in the well-known case (Reference 31) of the $N_2(v=1)$ and $CO_2(001)$ levels and in the less well-known case (Reference 32) of $O_2(v=1)$ and $CS_2(001)$. In the case of molecules in close resonance, our analysis suggests that an optimum mixture typically contains 0.2% of the infrared emitter and that most of the energy is stored in homonuclear molecules. Generally, the collisional relaxation of the homonuclear molecule in the pure gas is slow, as for N_2, H_2 and O_2, so that the added gas determines the rate of collisional deexcitation and thereby the fraction of the energy radiated before collisional deexcitation. Considerations such as these lead to the prediction that the largest signals will be obtained for D_2-CO mixtures. Smaller signals are expected for H_2-CO and D_2-CO_2 mixtures with the signals from H_2-CO_2 and O_2-CS_2 significantly lower because of faster collisional deexcitation. An important factor in the planning of our experiments is the availability, on a part-time basis, of a one-of-a-kind, very large area InSb detector for measurements of

the CO_2 and CO emission. The best detector we could purchase for the CS_2-O_2 measurements at 6.5 μm has a detectivity which is a factor of 30 smaller.

We have therefore emphasized the D_2 and H_2 experiments during the closing months of this contract period. The best way to summarize this work is to note that during the two months since the end of this contract period we have made an extensive series of measurements of the vibrational excitation of D_2 and H_2 using CO and CO_2 as the infrared emitters. Analyses of the data to determine vibrational excitation coefficients for H_2 and D_2 are now under way.

SECTION IV

CONCLUSIONS

The measurements of excitation coefficients for the production of free-free photons reported here serve to demonstrate the usefulness of simple theories for the calculation of free-free emission in gases. On the basis of this work and of theory and experiment at very high electron energies we have made predictions of free-free emission cross sections for several gases over a very wide range of electron energies. It would, of course, be desirable to test these predictions experimentally, particularly in the energy range of 20 to 100 eV where the poorly-known effect of inelastic collisions could result in increase of the cross section which we estimate to be about 20%. Experimental measurements at low electron energies in other gases would also be important.

The development and application of techniques for the measurement of rates of production of vibrationally excited homonuclear molecules is expected to provide important new information for use in the prediction of the characteristics of gas discharge devices and atmospheric plasmas. The work carried out during this contract period has recently led us to successful measurements of the vibrational excitation of H_2 and D_2 molecules. The production of these excited states is of particular current interest because of their importance in proposed negative ion sources and in switching devices.

REFERENCES

1. C. M. Lee, L. Kissel, R. H. Pratt, and H. K. Tseng, Phys. Rev. A 13, 1714 (1976); L. Kissel, C. MacCullem, and R. H. Pratt, "Bremsstrahlung energy spectra from electrons of kinetic energy 1 keV $\leq T \leq$ 2000 keV on neutral atoms $1 \leq Z \leq 92$," Sandia National Laboratories Report SAND81-1337, August 1981.

2. The momentum transfer cross sections used in Eq. (2) to obtain the solid curves of Fig. 1 were taken from M. Hayashi, "Recommended values of transport cross sections for elastic collision and total collision cross section for electrons in atomic and molecular gases," Report IPPJ-AM-19, Institute of Plasma Physics, Nagoya University, Nagoya, Japan.

3. S. Pfau and A. Rutscher, Z. Naturforsch. 22a, 2129 (1967) and Beitr. Plasmaphys. 8, 73 (1968); A. Rutscher and S. Pfau, Beitr. Plasmaphys. 8, 315 (1968) and Physica 81C, 395 (1976).

4. Yu. M. Kagan and N. N. Kristov, Opt. Spektrosk. 27, 710 (1969) [Opt. Spectrosc. 27, 388 (1969)]; Yu. B. Golubovskii, Yu. M. Kagan, and L. L. Komarova, Opt. Spektrosk. 34, 226 (1973) [Opt. Spectrosc. 34, 127 (1973)]; Yu. B. Golubovskii, Yu. M. Kagan, and L. L. Komanova, Opt. Spektrosk. 33, 1185 (1972) [Opt. Spectrosc. 33, 646 (1972)].

5. I. A. Vasileva, Yu. Z. Zhdavona, and A. Kh. Mnatsakanyan, Opt. Spektrosk. 29, 664 (1970) [Opt. Spectrosc. 29, 345 (1970)].

6. For a bibliography on free-free transitions in electron collisions with atoms and molecules see J. W. Gallagher, JILA Information Center Report No. 16, University of Colorado 1977 (unpublished).

7. R. L. Taylor and G. Caledonia, J. Quant. Spectrosc. Radiat. Transfer 9, 657 (1969); R. T. V. Kung and C. H. Chang, J. Quant. Spectrosc. Radiat. Transfer 16, 579 (1976).

8. C. G. Morgan, Rept. Progr. Phys. 38, 621 (1975). Note that absorption measurements have been made under the much more controlled conditions of an electron beam sustained discharge in H_2 and N_2 by S. Alroy and W. H. Christiansen, Appl. Phys. Lett. 32, 607 (1978). Also free-free transitions have been observed using laser radiation and monoenergetic electrons by D. Andrick and L. Langhans, J. Phys. B 9, L459 (1976).

9. O. B. Firsov and M. I. Chibisov, Zh. Eksp. Teor. Fiz. 39, 1770 (1960) [Sov. Phys.-JETP 12, 1235 (1961)].

10. V. Kas'yanov and A. Starostin, Zh. Eksp. Teor. Fiz. 48, 295 (1965) [Sov. Phys.-JETP 21, 193 (1965)].

11. T. Holstein, private communication and as quoted in Reference 12. Equations (18) and (19) of Reference 12 are too large by a factor of 2. Note that when Holstein's formula is used with Ashkin's total and momentum transfer cross sections the agreement with Ashkin's Q_{ff} is very good.

12. M. Ashkin, Phys. Rev. 141, 41 (1966).

13. S. Geltman, J. Quant. Spectrosc. Radiat. Transfer 13, 601 (1973). We are indebted to S. Geltman for tables of free-free transition matrix elements, which were interpolated to obtain the cross section values shown.

14. T. L. John and A. R. Williams, J. Phys. B 6, L384 (1973); M. S. Pindzola and H. P. Kelly, Phys. Rev. A 14, 204 (1976). See, however, J. R. Stallcop, Astron. Astrophys. 30, 293 (1974).

15. M. Gavrila and M. van der Wiel, Comments Atom. Mol. Phys. 8, 1 (1978); H. Krüger and M. Schulz, J. Phys. B 9, 1899 (1976). Resonance structure in the free-free scattering of electrons has been observed by L. Langhans, J. Phys. B 11, 2361 (1978).

16. S. A. Lawton and A. V. Phelps, J. Chem. Phys. 69, 1055 (1978).

17. K. Tachibana and A. V. Phelps, J. Chem. Phys. 75, 3315 (1981).

18. C. Yamabe and A. V. Phelps, J. Chem. Phys. (submitted).

19. L. M. Biberman and G. E. Norman, Usp. Fiz. Nauk 91, 193 (1967) [Sov. Phys. Uspekii 10, 52 (1967)].

20. L. S. Frost and A. V. Phelps, Phys. Rev. 127, 1621 (1962); ibid. 136, A1538 (1964).

21. R. Winkler, P. Michel, and J. Wilhelm, Beit. Plasmaphys. 18, 31 (1978).

22. S. Pfau, A. Rutscher, and R. Winkler, Beit. Plasmaphys. 16, 317 (1976).

23. The data shown in Fig. 5 from Reference 4 are those for which electron-electron collisions effects are negligible, i.e., for the largest value of pR and the smallest value of i/R in their notation.

24. Evidence for free-free emission has been obtained from measurements of electroluminescence from scintillation counters filled with Xe at densities near 6×10^{26} m^{-3} and operated at E/N of less than 5×10^{-23} Vm^2. See Yu. A. Butikov, B. A. Polgoshain, V. N. Lebedenko, A. M. Rogoshin, and B. V. Rodionov, Zh. Eksp. Teor. Fiz. 57, 42 (1969) [Sov. Phys.-JETP 30, 24 (1970)].

25. V. M. Atrazhev and I. T. Yakubov, Teplofiz. Vys. Temp. 18, 1292 (1980) [High Temperature 18, 966 (1980)]; G. L. Braglia and V. Dallacasa, in Electron and Ion Swarms, edited by L. G. Christophorou (Pergamon, New York, 1981), p. 83; G. R. Freeman, ibid., p. 93.

26. A. Garscadden and W. F. Bailey, International Symposium on Rarefied Gas Dynamics, July 1980, Charlottesville, NC. To be published in *Progress in Astronautics and Aeronautics* (1981).

27. H. Ehrhardt, L. Langhans, F. Linder, and H. S. Taylor, Phys. Rev. 173, 222 (1968).

28. R. W. Crompton, D. K. Gibson, and A. G. Robertson, Phys. Rev. A 2, 1386 (1970).

29. A. G. Englehardt and A. V. Phelps, Phys. Rev. 131, 2115 (1964).

30. F. Linder and H. Schmidt, Z. Naturforsch. A 26, 1617 (1971).

31. B. R. Bulos and A. V. Phelps, Phys. Rev. A 14, 615 (1976).

32. Few data are available regarding the kinetics of vibrationally excited CS_2. Our estimates are scaled from similar molecules, such as CO_2. CS_2 deactivation is discussed by J. K. Hancock, D. F. Starr, and W. H. Green, J. Chem. Phys. 61, 3017 (1974).

*USGPO: 1983-659-063-044